Technical Report

Evolution of frictional shear resistance in response to rapid variations of normal stress

SCEC Award # 21088

Principal Investigator: Ares Rosakis, California Institute of Technology

1. Summary of the results

Friction formulations typically assume shear resistance to be proportional to normal stress. However, when normal stress changes rapidly enough, frictional shear resistance no longer obeys proportionality to the normal stress but rather evolves with slip gradually (Prakash and Clifton, 1993). In this project, we investigate the evolution of shear stress in response to rapid normal stress variations using laboratory experiments of spontaneously propagating dynamic ruptures. Our experiments produce variations in fault-normal stress due to the interaction of dynamic rupture with the free surface, similarly to what occurs in natural thrust events (Gabuchian et al., 2014; 2017). Our experimental measurements clearly demonstrate the delay between normal stress changes and the corresponding changes in frictional resistance, with important implications for the dynamics of thrust earthquakes near the free surface. The experiments make use of full-field measurements of displacements, strains, and stresses by combining digital image correlation (DIC) technique with ultrahigh-speed photography (Rubino et al., 2016; 2017; 2019; 2020), which thoroughly characterize rupture interaction with the free surface, including the large normal stress reductions. Our full-field measurement capability allows us to confirm and quantify the asymmetry between the experimental motions of the hanging and footwalls, with larger velocity magnitudes occurring at the hanging wall. Interestingly, because the motion of the hanging wall is generally near-vertical, while that of the footwall is at dip direction shallower than the dip angle of the fault, the horizontal surface velocity components are found to be larger at the footwall than at the hanging wall.

1. Project motivation and objective

The delayed in response of frictional shear resistance to variations in normal tractions, and its proper representation in friction formulations, is critically important for investigations of several key earthquake source problems, including (i) slip on locally rough/nonplanar interfaces, a topic of particular interest in SCEC5 (Dieterich and Smith, 2009; Fang et al., 2011; Dunham et al., 2011; Duru and Dunham, 2016); (ii) the dynamics of ruptures on thrust and normal faults near the Earth's surface, which is important for near-fault shaking and tsunami generation, and which contains rapid changes in the fault-normal stress due to the interaction of rupture with the free surface (e.g., Oglesby et al. 1998; Nielsen, 1998; Oglesby et al., 2000; Madariaga, 2003; Duan and Oglesby, 2005; Ma and Beroza, 2008; Kozdon and Dunham, 2014; Gabuchian et al., 2014; 2017), (iii) dynamic rupture on faults separating crustal rocks with different elastic properties, a common case for mature strike-slip faults that have slipped many kilometers, which causes rapid fault-normal stress changes due to coupling between the fault normal stress and slip (e.g., Andrews and Ben-Zion, 1997; Cochard et al., 2000; Rice et al., 2001; Xia et al., 2005; Shi and Ben-Zion, 2006; Rosakis et al., 2007; Bhat et al., 2010; Shlomai and Finberg, 2016), and (iv) shear-heating-induced rapid pressurization of pore fluids during seismic slip, which potentially results in rapid enough effective normal stress changes (e.g., Lachenbruch, 1980; Mase and Smith, 1985; Rice, 2006; Schmitt et al., 2011).

In this project, we use laboratory experiments to investigate the evolution of shear stress in response to rapid normal stress variations in order to achieve the following goals:

- Study the normal stress variations and the corresponding shear resistance evolution produced by the propagation of spontaneous ruptures near a free surface for a broad range of experimental parameters, comprising both supershear and sub- Rayleigh ruptures;

- Explore the dependence of frictional parameters on normal stress to improve our ability to reproduce the measured friction behavior under a wide range of conditions.
- Investigate the effects of asymmetric geometry and heterogeneous frictional resistance on the ground motion and study the decay away from the fault.

2. Relevance of the project goals to the objectives of SCEC

This project addresses the following SCEC5 Research Priorities:

P4.a. Determine the relative roles of fault geometry [and] heterogeneous frictional resistance, […] in controlling and bounding ground motions.

P1.d. Quantify stress heterogeneity on faults at different spatial scales.

P3.g. Assess the importance of the mechanical properties of the near-surface.

Our experiments featuring spontaneously propagating ruptures reaching the free surface, performed under a range of experimental parameters, will contribute to determine the relative roles of fault geometry and frictional resistance in controlling and bounding ground motion, and thus address **P4.a**. Our measurements of shear stress in the near-surface region will also contribute to **P1.d** and **P3.g**.

3. Results

Friction response to rapid normal stress variations is key to study of several problems in earthquake source science, as discussed in section 1. We study this problem in a highly instrumented experimental setup that produces variations in fault-normal stress due to the interaction of dynamic rupture with the free surface. The lab earthquake setup features a dynamic rupture along an inclined, frictional interface formed by two compressed quadrilateral sections of Homalite (Figure 1). The full-field imaging technique that we have developed enables to image the motions and stress changes within a field of view (FOV) close to the free surface. It allows us to both obtain the dynamic details of the phenomenon as well as image the evolution of fault-normal stress, fault-parallel shear stress, and hence friction along the interface close to the free surface, and hence to study how friction evolves under the conditions of rapid normal stress variations and to distinguish between different proposed formulations. We have already been successful to characterize dynamic friction evolution in the bulk and used friction laws to describe its behavior (Rubino et al., 2017).

The motions and stress changes close to the free surface are adequately resolved by the full-field imaging technique that we have developed (Rubino et al., 2019; Tal et al., 2019). Accurate measurements of stresses near the interface are very important when digital image correlation (DIC) is applied to study the dynamics of laboratory frictional rupture. However, DIC algorithms involve small errors that can lead to non-physical discontinuities in the stress field across the interface. Using a previous SCEC award, we have developed an algorithm to locally adjust the displacements computed by DIC near frictional interfaces, such that local stress fields satisfy the continuity of traction across the interface (Tal et al., 2019).

Over the last funding period we have studied the effect of rapid normal stress variations over a broad range of experimental conditions. We also investigated the effects of asymmetric geometry and heterogeneous frictional resistance on the ground motion and studied the decay away from the fault.

Our full-field measurement capability allows us to confirm and quantify the asymmetry between the experimental motions of the hanging and footwalls, with larger velocity magnitudes occurring at the hanging wall. Plots of the time histories of slip rate, $\dot{\delta}$, at different locations along the fault (Figure 2a) provide further insight into the effect of the free surface on the rupture process itself. At the largest distance from the free surface (x_f = 13.5 mm), there are two separated peaks in $\dot{\delta}$ that correspond to the arrival ($\dot{\delta} = 6.5$ m/s at t = 54 μs) and reflection ($\dot{\delta} = 9$ m/s at t = 69 μs) of the supershear rupture. As the distance to the free surface decreases, the peaks of arrival and reflection merge together, with a transition into a single peak of $\dot{\delta} = 12.5$ m/s near the free surface (x_f = 1.5 mm). The trailing-Rayleigh rupture shows a clear peak of $\dot{\delta} = 9.5$ m/s at x_f = 1.5 mm, but as x_f increases, the peak becomes smaller and wider, with a weak signal at x_f = 13.5 mm.

Experiments under lower compressive loads are characterized by weaker ruptures with smaller slip rates. The ruptures show similar characteristics to those described above, featuring a supershear rupture in the front followed by a trailing Rayleigh rupture. However, as P decreases, there is a transition from a dominant supershear rupture to a dominant trailing Rayleigh rupture. In Exp. #4, which was conducted under the lowest compressive load of P = 4.9 MPa (Figure 2b), the peak slip rate of the supershear rupture near the free surface (x_f = 1.5 mm) is $\dot{\delta} = 2.8$ m/s, while that of the trailing Rayleigh is $\dot{\delta} = 5$ m/s. Moreover, there is a delay of ~5 μs in the arrival of the supershear rupture to FOV compared to Exp. #1 because of a slightly slower rupture speed of V_r = 2 km/s = 1.57c_s and a larger transition distance of 12.8 mm.

Snapshots of the of full-field particle velocity magnitude, $|\dot{\mathbf{u}}|$, with overlaid velocity vectors on the fault and on the free surface, during different stages of Exp. #1 (Figure 1), shed light on the dynamics of the supershear rupture and the subsequent trailing Rayleigh rupture during the interaction with the free surface, as well as their effects on the ground motion. The supershear rupture (Figure 4, top panels) approaches the free surface (t = 57 μs) with a peak particle velocity magnitude of 4 m/s and transition from a dominant fault-normal particle motion ahead of the rupture front to a fault-parallel particle motion behind it. Correspondingly, at the surface, the right part of the hanging wall, which is already behind the rupture front, moves parallel to the fault with a velocity magnitude of $|\dot{\mathbf{u}}|, = 2$ m/s. The surface velocities, $\dot{\mathbf{u}}_s$, decrease and rotate in locations on the surface that are ahead the rupture front (decreasing x_1). During the interaction of the rupture with the free surface (t = 63 μs), $|\dot{\mathbf{u}}|$ increases and becomes asymmetric with respect to the fault, with peak values of 8 and 4.5 m/s at the hanging and foot walls, respectively. The walls slide in opposite directions, with small deviations from the orientation of the fault. After the rupture is reflected from the free surface (t = 78 □s), sliding continues at smaller particle velocities, with a sub-vertical motion of the hanging wall and motion at a dip of $\beta \approx 40°$ of the footwall. At this stage, the magnitude of accumulated surface displacements, $|\mathbf{u}_s|$, on the hanging wall ranges between $|\mathbf{u}_s| = 100$ μm near the fault and $|\mathbf{u}_s| = 90$ μm at $x_1 = 5$ mm, while that on the footwall ranges between $|\mathbf{u}_s| = 74$ μm near the fault and $|\mathbf{u}_s| = 65$ μm at $x_1 = -5$ mm (Figure 3).

Consistent with field observations and numerical models, the experimental surface motions show asymmetry between the hanging and footwalls during the interaction of both the supershear and the trailing Rayleigh ruptures with the free surface, with larger velocity magnitudes at the hanging wall. However, for the dip angle of $\beta = 61°$ considered in our experiments, the motion of the hanging wall is generally a nearly-vertical motion, while that of the footwall is at a dip direction which is shallower than the dip angle of the fault. That leads to larger horizontal surface velocities at the footwall than at the hanging wall. The attenuation in surface velocity with distance from the fault is generally larger at hanging wall than at the footwall and for the vertical component than for the horizontal one.

Publications

Tal, Y., Rubino, V., A. J. Rosakis, and N. Lapusta, Dynamics and near-field surface motions of transitioned supershear laboratory earthquakes in thrust faults, *Journal of Geophysical Research* (accepted), 2022.

Tal, Y., Rubino, V., A. J. Rosakis, and N. Lapusta, Illuminating the physics of dynamic friction through laboratory earthquakes on thrust faults, *Proceedings of the National Academy of Sciences*, 117(35), 21095-2100 , 2020. https://doi.org/10.1073/pnas.2004590117

Presentations

Rubino, V., Y. Tal, A. J. Rosakis, and N. Lapusta, Experimental study of frictional shear resistance under rapid variations of normal stress and near-field ground motion of thrust earthquakes, *Southern California Earthquake Center (SCEC) Annual Meeting* (held virtually), September 1-3, 2021.

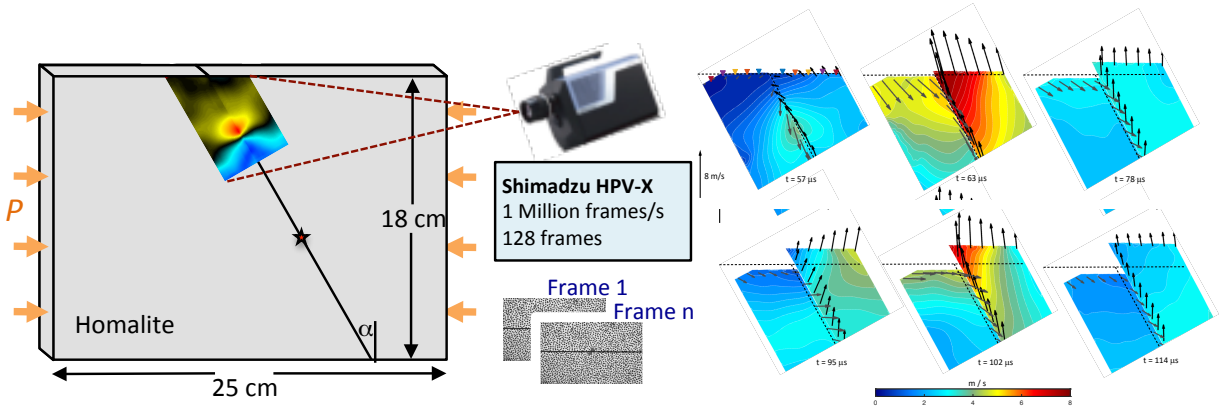

Figure 1. Experimental setup. Dynamic shear ruptures are initiated by a small burst of a NiCr wire at distance $x_f = 11.5$ cm from the free surface and propagate spontaneously along a frictional interface inclined at a dip angle $\beta = 61^o$ between two Homalite plates, which are loaded under a compressional load P. An ultrahigh-speed camera system (Shimadzu HPV-X) is used to record 128 images of a target area of 19 x 12 mm^2 near the free surface at a rate of 1 million frames/second. The images are analyzed with the digital image correlation method to obtain full-field displacement and velocity fields. Panels on the right: Snapshots of the particle velocity magnitude at different stages of Exp. #1 (P = 15 MPa), with overlaid vectors showing the direction and magnitude of particle velocities near the interface and at the free surface. The deformation is exaggerated by a factor of 10. Modified from Tal et al., 2022.

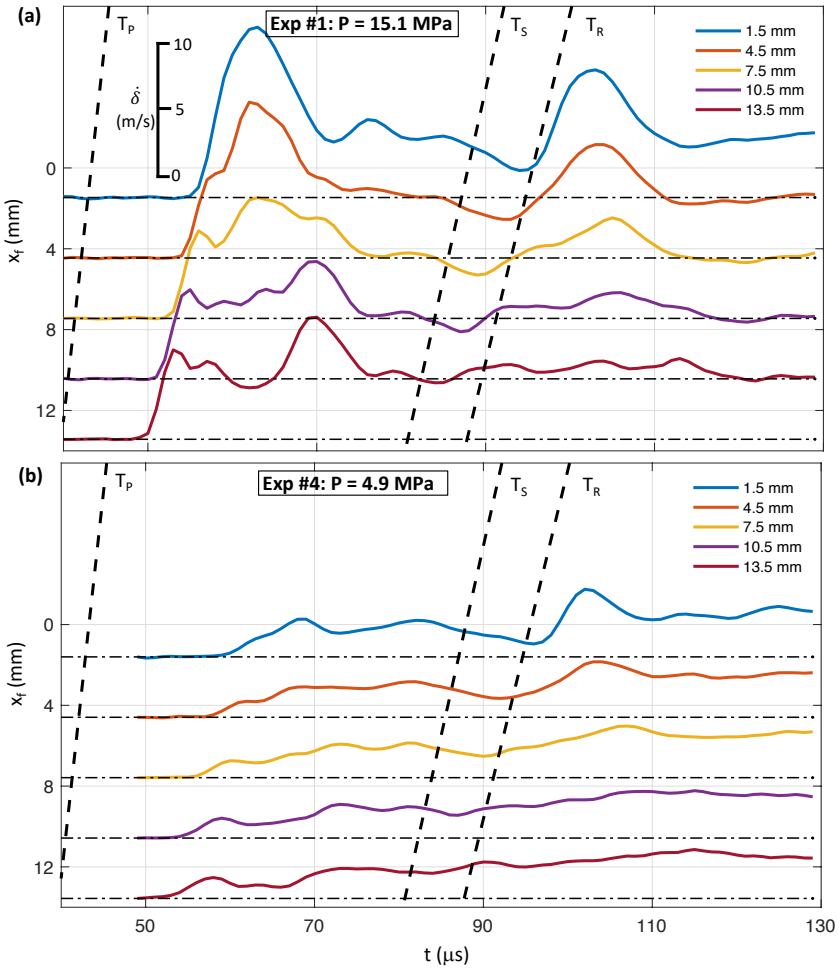

Figure 2. Slip rate vs. time at five locations on the fault with different distances (x_f) from the free surface for (a) Exp #1 (P = 15 MPa) and (b) Exp #4 (P = 4.9 MPa). The locations are shown in the Figure 2. Dashed lines marked with T_p, T_s, and T_R indicate the arrival times of P, S, and Rayleigh waves. Note that the peaks in $\dot{\delta}$ increase near the free surface for both the supershear rupture and the trailing Rayleigh. The lower level of applied loading P in Exp #4 results in a weaker rupture with smaller slip rates. Modified from Tal et al., 2022.

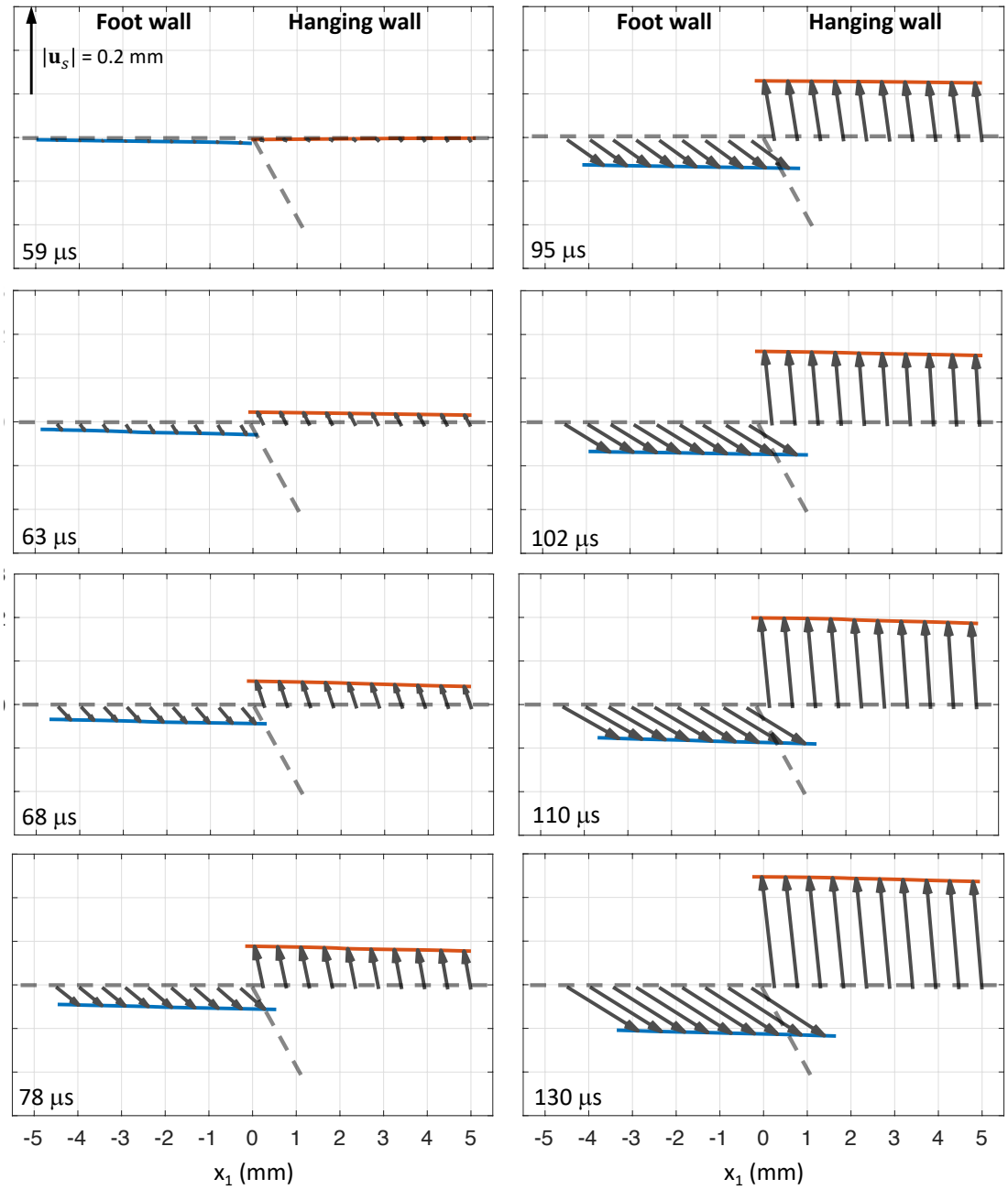

Figure 3. Snapshots of accumulated displacements along the surface, $\mathbf{u}_s$, at different stages of Exp. #1 (P = 15 MPa). The vector sizes are amplified by a factor of 10. The left (t = 59 – 78 μs) and right (t = 95 – 130 μs) panels capture the interactions of the supershear and trailing Rayleigh ruptures with the free surface, respectively. The figure highlights the differences in $|\mathbf{u}_s|$ between the hanging and footwalls, as well as the rotations of $\mathbf{u}_s$ throughout the experiment into motions that are nearly-vertical at the hanging wall and at a dip of $\beta \approx 32°$ at the footwall. Modified from Tal et al., 2022.

References

Andrews, D. J., Y. Ben-Zion, Wrinkle-like slip pulse on a fault between different materials, *J. Geophys. Res. Solid Ea*. **102** (B1), 553-571, 1997.

Bhat, H. S., R. L. Biegel, A. J. Rosakis, C. G. Sammis, The effect of asymmetric damage on dynamic shear rupture propagation II. With misatch in bulk elasticity, *Tectonophysics* **493**, 263-271, 2010.

Brown, K. M., Y. Fialko, Melt welt" mechanism of extreme weakening of gabbro at seismic slip rates, *Nature* **488**, 638–641, 2012.

Cochard, A. and J. R. Rice, Fault rupture between dissimilar materials. Ill-posedness, regularization, and slip-pulse response, *J. Geophys. Res.* **105** (B11), 25891-25907, 2000.

Dieterich J.H., and D.E. Smith, Nonplanar faults: Mechanics of slip and off-fault damage, **166**(1799-1815), 2009.

Duan, B. and D. D. Oglesby, Multicycle dynamics of nonplanar strike-slip faults, *J. Geophys. Res.* **110** (B3), 1-16, 2005.

Duru, K. and E. M. Dunham, Dynamic earthquake rupture simulations on nonplanar faults embedded in 3D geometrically complex, heterogeneous elastic solids, *J. Comput. Phys.* **110** (B3), 1-16, 2005.

Dunham, E. M., D. Belanger, L. Cong, and J. E. Kozdon, Earthquake ruptures with strongly rate-weakening friction and off-fault plasticity, 2: Nonplanar faults, *Bulletin of the Seismological Society of America*, **101**(5), 2308-2322, 2011.

Fang, Z., J.H. Dieterich, K.B. Richards-Dinger, and G. Xu, Earthquake nucleation on faults with nonconstant normal stress, **116**(B09307), 2011.

Gabuchian, V., A. J. Rosakis, N. Lapusta, and D. Oglesby, Experimental investigation of strong ground motion due to thrust fault earthquakes, *J. Geophys. Res.* **119** (2), 1316-1336, 2014.

Gabuchian, V., Rosakis, A. J., Bhat, H., Madariaga, R. and Lapusta, N., Experimental evidence that thrust earthquake ruptures might open faults, *Nature* **545,** 336-340, 2017.

Kozdon, J. E. and E. M. Dunham, Constraining shallow slip and tsunami excitation in megathrust ruptures using seismic and ocean acoustic waves recorded on ocean-bottom sensor networks, *Earth and Planetary Science Letters*, **396**, 56-65, 2014

Ma, S., G. C. Beroza, Rupture dynamics on a bimaterial interface for dipping faults, *Bull. Seismol. Soc. Am.* **98** (4), 1642-1658, 2008.

Madariaga, R., Radiation from a Finite Reverse Fault in a Half Space, *Pure Appl. Geophys.* **160**, 555-577, 2003.

Mase, C. W. and L. Smith, Pore–fluid pressures and frictional heating on a fault surface, *Pure Appl. Geophys*. **122**, 583–607, 1985.

Nielsen, S. B., Free surface effects on the propagation of dynamic rupture, *Geophys. Res. Lett.* **25** (1), 125-128, 1998.

A. Niemeijer, G. Di Toro, S. Nielsen, F. Di Felice, Frictional melting of gabbro under extreme experimental conditions of normal stress, acceleration, and sliding velocity. *J. Geophys. Res. Solid Earth* 116, B07404, 2011.

Oglesby, D. D., R. J. Archuleta, and S. B. Nielsen, Earthquakes on Dipping Faults. The Effect of Bronken Symmetry, *Science* **280** (5366), 1055-1059, 1998.

Oglesby, D. D., R. J. Archuleta, and S. B. Nielsen, The Three-Dimensional Dynamics of Dipping Faults, *Bull. Seimol. Soc. Am.* **90** (3), 616-628, 2000.

Prakash, V., and R. J. Clifton, Time resolved dynamic friction measurements in pressure-shear, *Experimental Techniques in the Dynamics of Deformable Solids*, Applied Mechanics Div. Vol. 165 (AMD-Vol. 165). American Society of Mechanical Engineers, New York, pp. 33-48, 1993.

Rice, J. R., N. Lapusta, K. Ranjith, Rate and state dependent friction and the stability of sliding between elastically deformable solids, *J. Mech. Phys. Solids* **49** (9), 1865-1898, 2001.

Rice, J. R., Heating and weakening of faults during earthquake slip, *J. Geophys. Res*., **111** (B5), 1-29, 2006.

Rosakis, A. J., K. Xia, G. Lykotrafitis and H. Kanamori, Dynamic Shear Rupture in Frictional Interfaces. Speeds, Directionality and Modes, *Treatise Geophys.* **4**, 153-192, 2007.

Rubino, V., A. J. Rosakis, and N. Lapusta, Dynamic visualization of supershear ruptures, *XXIV ICTAM*, Montreal, Canada, August 21-26, 2016.

Rubino, V., A. J. Rosakis, and N. Lapusta, Understanding dynamic friction through spontaneously evolving laboratory earthquakes, *Nature Communications*, 8:15991, 2017.

Rubino, V.; Rosakis, A.J.; Lapusta, N. Full-field ultrahigh-speed quantification of dynamic shear ruptures using digital image correlation. *Exp. Mech*, 59(5), 551-582, 2019.

Rubino, V., A.J. Rosakis and N. Lapusta, Spatiotemporal properties of sub-Rayleigh and supershear ruptures inferred from full-field dynamic imaging of laboratory experiments, *Journal of Geophysical Research: Solid Earth,* 125, e2019JB01892, 2020.

Saffer, D. M. & Marone, C. Comparison of smectite-and illite-rich gouge frictional properties: application to the updip limit of the seismogenic zone along subduction megathrusts. *Earth Planet. Sci. Lett.* **215,** 219–235, 2003.

Schmitt, S.V., P. Segall, T. Matsuzawa, Shear heating-induced thermal pressurization during earthgquake nucleation, *J. Geophys. Res*. **116**, B06308, 2011.

Shi, Z., Y. Ben-Zion, A. Needleman, Properties of dynamic rupture and energy partition in a solid with a frictional interface, *J. Mech. Phys. Solids* **56** (1), 5-24, 2008.

Shlomai, H. and J. Fineberg, The structure of slip-pulses and supershear ruptures driving slip in bimaterial friction, *Nature Communications* **7** (11787), 2016.

Tal, Y., Rubino, V., A. J. Rosakis, and N. Lapusta, Studying the shear resistance response to rapid normal-stress variations near the free surface on experimental thrust faults, *SSA meeting*, Miami, Florida, USA, May 14-17, 2018.

Tal, Y., Rubino, V., A. J. Rosakis, and N. Lapusta (2019) Enhanced Digital Image Correlation Analysis of Ruptures with Enforced Traction Continuity Conditions Across Interfaces. *Applied Sciences*, 9 (8). Art. No. 1625. ISSN 2076-3417.

Tal, Y., Rubino, V., A. J. Rosakis, and N. Lapusta, Illuminating the physics of dynamic friction through laboratory earthquakes on thrust faults, *Proceedings of the National Academy of Sciences*, 117(35), 21095-2100 , 2020.

Tal, Y., Rubino, V., A. J. Rosakis, and N. Lapusta, Dynamics and near-field surface motions of transitioned supershear laboratory earthquakes in thrust faults, *Journal of Geophysical Research* (accepted), 2022.

Xia, K., A. J. Rosakis, H. Kanamory, and J. R. Rice, Laboratory Earthquakes Along Inhomogeneus Faults. Directionality and Supershear, *Science* **308** (5722), 681-684, 2005.